

Hydrogen isotope exchange between *n*-alkanes and water under hydrothermal conditions

Eoghan P. Reeves^{a,b,*,1}, Jeffrey S. Seewald^b and Sean P. Sylva^b

^a*MIT/WHOI Joint Program in Oceanography*

^b*Department of Marine Chemistry and Geochemistry, Woods Hole Oceanographic Institution,
360 Woods Hole Road, Woods Hole, MA 02543, USA*

*Corresponding author.

Tel.: +49 4212 1865416

Email address: reeves@uni-bremen.de, ereeves@whoi.edu (E.P. Reeves)

¹Present address: MARUM Center for Marine Environmental Sciences & Department of Geosciences, University of Bremen, 2 Klagenfurter Strasse, 28359 Bremen, Germany

Manuscript W8245, re-submitted with minor revisions to

Geochimica et Cosmochimica Acta, 03/10/2011

Abstract

To investigate the extent of hydrogen isotope (^2H and ^1H) exchange between hydrocarbons and water under hydrothermal conditions, we performed experiments heating $\text{C}_1\text{--C}_5$ *n*-alkanes in aqueous solutions of varying initial $^2\text{H}/^1\text{H}$ ratios in the presence of a pyrite-pyrrhotite-magnetite redox buffer at 323°C and $35\text{--}36\text{MPa}$. Extensive and reversible incorporation of water-derived hydrogen into $\text{C}_2\text{--C}_5$ *n*-alkanes was observed on timescales of months. In contrast, comparatively minor exchange was observed for CH_4 . Isotopic exchange is facilitated by reversible equilibration of *n*-alkanes and their corresponding *n*-alkenes with H_2 derived from the disproportionation of water. Rates of $\delta^2\text{H}$ variation in C_{3+} *n*-alkanes decreased with time, a trend that is consistent with an asymptotic approach to steady-state isotopic compositions regulated by alkane-water isotopic equilibrium. Substantially slower $\delta^2\text{H}$ variation was observed for ethane relative to $\text{C}_3\text{--C}_5$ *n*-alkanes, suggesting that the greater stability of C_{3+} alkenes and isomerization reactions may dramatically enhance rates of $^2\text{H}/^1\text{H}$ exchange in C_{3+} *n*-alkanes. Thus, in reducing aqueous environments, reversible reaction of alkenes and their corresponding alkanes facilitates rapid $^2\text{H}/^1\text{H}$ exchange between alkyl- and water-bound hydrogen on relatively short geological timescales at elevated temperatures and pressures. The proximity of some thermogenic and purported abiogenic alkane $\delta^2\text{H}$ values to those predicted for equilibrium $^2\text{H}/^1\text{H}$ fractionation with ambient water suggests that this process may regulate the $\delta^2\text{H}$ signatures of some naturally occurring hydrocarbons.

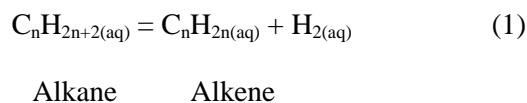
1. INTRODUCTION

Stable hydrogen isotope measurements of carbon-bound hydrogen ($H = {}^1H$ and 2H) at a compound-specific level have become widespread in organic geochemical investigations in recent years. Hydrogen isotope compositions of *n*-alkanes have been utilized to examine such diverse processes as abiogenic hydrocarbon formation (Sherwood Lollar et al., 2002; Fu et al., 2007; Proskurowski et al., 2008; McCollom et al., 2010), formation and biodegradation of petroleum constituents (Schoell, 1983; Whiticar et al., 1985; Tang et al., 2005; Schimmelmann et al., 2006; Boreham et al., 2008; Liu et al., 2008; Wang et al., 2009a; Burruss and Laughrey, 2010) and paleoenvironmental changes (Schefuss et al., 2005; Sachse et al., 2006; Eglinton and Eglinton, 2008). The use of δ^2H measurements to infer primary kinetic or equilibrium isotopic effects associated with molecule formation implicitly assumes that organic hydrogen is resistant to secondary modification over pertinent geologic timeframes. There is growing evidence to suggest that exchange or incorporation of water-derived hydrogen (H) into organic molecules can obscure primary isotopic signatures (Sessions et al., 2004; Schimmelmann et al., 2006) but the processes involved are poorly understood.

Although numerous experimental studies have examined ${}^2H/{}^1H$ exchange between high molecular weight organic matter (e.g. kerogen and oil) and ambient water at elevated temperatures (see Schimmelmann et al. (2006) for review), limited information exists for low molecular weight hydrocarbons such as the C_1 to C_5 *n*-alkanes. These hydrocarbons represent an important class of compounds in a variety of high and low temperature environments and their isotopic composition may provide information regarding formation processes. For example, δ^2H trends as a function of carbon number have been used to infer mechanistic information regarding hydrocarbon abiogenesis in Precambrian rocks of the Canadian Shield (Sherwood Lollar et al., 2002), and may allow identification of similar abiogenic processes that have been postulated to occur during serpentinization of ultramafic igneous crust (Berndt et al., 1996; McCollom and Seewald, 2001, 2007; Fu et al., 2007; Proskurowski et al., 2008). In addition, C_1 to C_5 *n*-alkanes

are abundant in petroleum formed by thermal maturation of sedimentary organic matter (Tissot and Welte, 1984; Hunt, 1996) and the importance of natural gas as an energy source is increasing, leading to the exploitation of more unconventional gas accumulations. Hydrogen isotope measurements of natural gases have recently been examined in combination with quantum chemical considerations to evaluate $^2\text{H}/^1\text{H}$ ratios as proxy indicators of thermal maturity (Tang et al., 2007; Ni et al., 2011). In the case of both thermogenic and abiogenic low molecular weight hydrocarbons, it is typically assumed that trends in $\delta^2\text{H}$ values with carbon chain length are regulated by kinetic isotope effects during molecule formation. However, the susceptibility of low molecular weight *n*-alkanes to $^2\text{H}/^1\text{H}$ exchange in water-rich, high temperature environments is unclear and must be constrained in order to understand observed isotopic compositions.

Water is ubiquitous in both hydrothermal and petroleum-producing sedimentary basins and may be a reactive source of H not just during the generation of petroleum hydrocarbons, but also during subsequent migration and accumulation processes (Lewan, 1997; Seewald, 2003; Schimmelmann et al., 2006). Although aliphatic H is typically considered to be the most isotopically conservative moiety under low temperature conditions (Schimmelmann et al., 2006), aqueous reaction paths at elevated temperatures could facilitate reversible exchange with water-derived H. Experiments conducted under hydrothermal conditions (300–350°C, 35MPa) with short chain *n*-alkanes have shown that these compounds and their corresponding *n*-alkenes may rapidly attain reversible states of redox-dependent metastable equilibrium according to the following reaction (Seewald, 1994, 2001a, 2003):



Given that aqueous H_2 may be derived from the reversible disproportionation of water, reaction (1) represents a viable pathway for reversible $^2\text{H}/^1\text{H}$ exchange between water and the *n*-alkane molecule. In this study we examine the rate and extent of reversible $^2\text{H}/^1\text{H}$ exchange between

dissolved C₁ to C₅ *n*-alkanes and water at hydrothermal conditions by this mechanism and the implications for both thermogenic and purported abiogenic hydrocarbon $\delta^2\text{H}$ values.

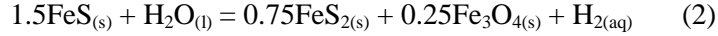
2. METHODS

2.1 Experimental Approach and Setup

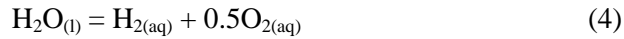
All experiments were conducted by heating dissolved mixtures of C₁ to C₅ *n*-alkanes in aqueous solutions of varying ²H/¹H ratios within a flexible cell hydrothermal apparatus (Seyfried et al., 1979; Seyfried, 1987). The apparatus consists of a gold reaction cell equipped with titanium fittings and a capillary exit tube and sampling valve. The reaction cell is contained within a stainless steel pressure vessel that allows external control of pressure. The capillary exit tube and valve can be used to remove fluids for chemical analysis or modify reaction cell contents by injection of solutions, without perturbing the temperature and pressure of the experiment. Rapid cooling of removed aliquots to room temperature also minimizes retrograde reactions that can occur during prolonged quenching. Prior to use, the titanium surfaces in contact with the reaction cell contents were heated in air for 24h at 400°C to form an inert TiO₂ surface layer. This apparatus has been used in numerous investigations of aqueous low molecular weight organic compounds under hydrothermal conditions (Seewald, 1994, 2001a; Horita and Berndt, 1999; McCollom and Seewald, 2001, 2003a, 2003b; Foustoukos and Seyfried, 2004; Seewald et al., 2006; Fu et al., 2007; McCollom et al., 2010) and both Au and TiO₂ are considered the least reactive surfaces that can fulfill the requirements of the apparatus (Palmer and Drummond, 1986; Bell et al., 1994; McCollom and Seewald, 2003a, 2003b).

Laboratory experiments have demonstrated that the stability of aqueous low molecular weight *n*-alkanes is highly sensitive to the redox state of the fluid (Seewald, 1994, 2001a). Hence, to demonstrate that variations in *n*-alkane ²H/¹H ratios are attributable to reversible ²H/¹H exchange with water rather than kinetic isotope effects associated with degradation and/or side reactions, it is crucial that the extent to which these latter reactions occur is limited. Seewald (2001a) demonstrated that observed rates of *n*-heptane degradation by stepwise aqueous oxidation varied dramatically depending on the mineral redox buffer employed. Of the three buffers used (pyrite-pyrrhotite-magnetite (PPM), hematite-magnetite-pyrite (HMP) and hematite-magnetite

(HM)), *n*-alkane degradation was slowest with the more reducing PPM mineral assemblage (Seewald, 2001a). Hence, this buffer was chosen for all experiments (Figure 1). The PPM assemblage buffers both $H_{2(aq)}$ and $H_2S_{(aq)}$ activities ($a_{H_2(aq)}$ and $a_{H_2S(aq)}$, respectively) via the following chemical reactions:



The influence of this mineral assemblage on the oxidation state of the fluid is reflected in the abundance of dissolved H_2 , which is directly related to the aqueous O_2 activity by the disproportionation of water (or reverse Knallgas reaction), which rapidly attains thermodynamic equilibrium at high temperatures:



The effectiveness of the PPM mineral assemblage in buffering dissolved H_2 and H_2S concentrations on short (weekly) timescales has been demonstrated in numerous previous experiments (Seewald, 1994, 1997, 2001a; McCollom and Seewald, 2003b). Accordingly, aqueous H_2S was not routinely measured to conserve the limited quantities of fluid in the reaction cell. In addition to the above practical considerations, the choice of the PPM assemblage also reflects a reasonable redox state within the range encountered in seafloor hydrothermal systems (Shock, 1992; Seyfried and Ding, 1995; Seyfried et al., 2004) and provides a source of S for the potential formation of catalytic S species that may facilitate organic reactions (Seewald, 2001a). We cannot exclude the possibility of unknown catalysis of aqueous organic reactions by the assemblage minerals during our experiments. All three minerals are, however, found associated with oil/gas deposits (Surdam and Crossey, 1985; Reynolds et al., 1990; Liu and Liu, 1999; Aubourg and Pozzi, 2010) and in hydrothermal settings (Shock, 1992). Hence, the assemblage used in our experimental design does not necessarily provide mineral surfaces beyond those already existing in these environments.

Each experiment contained ~15g of a homogeneous mixture of commercially synthesized (>99.99% pure, Puratronic®) pyrite, pyrrhotite and magnetite powders (~5g each) and ~30g water of a given $\delta^2\text{H}_{\text{H}_2\text{O}}$ value. ^2H -enriched and ^2H -depleted aqueous solutions were made with dilutions of 99wt.% $^2\text{H}_2\text{O}$ and ^2H -depleted water (Cambridge Isotope Labs) in Milli-Q water, respectively. Both starting solutions contained a low but known concentration of NaCl to facilitate detection of reaction cell leakage. Prior to pressurization of the reaction cell, the reaction cell gas headspace (~10mL) was purged with Ar to remove O_2 , partially evacuated, and then loaded with a gaseous mixture of C_1 to C_5 *n*-alkanes of known $\delta^2\text{H}$ with approximately equimolar carbon amounts per *n*-alkane. Because hydrocarbon concentrations initially loaded into each reaction cell were not measured, concentrations at the start of each experiment cannot be directly constrained. However, the relatively slow changes in concentrations of C_1 to C_5 *n*-alkanes suggests that the initial experimental compositions were not substantially different from values measured during the first sampling events. By including CH_4 in the dissolved gas mixture, H exchange involving an *n*-alkane that cannot form an alkene could be examined relative to the C_{2+} *n*-alkanes. A small amount (<1.5g) of starting solution was then injected to completely flush the gas mixture into the reaction cell for subsequent dissolution during pressurization and heating. It has been demonstrated that commercial minerals of the purity used here contain trace carbon impurities that are typically released during the early stages of an experiment (Seewald, 1994, 2001a; McCollom and Seewald, 2003a, 2003b). As a result, C_1 to C_5 *n*-alkane concentrations in each experiment were intentionally >2 orders of magnitude larger than any contaminant hydrocarbon concentrations observed in previous studies to ensure observed *n*-alkane $\delta^2\text{H}$ values ($\delta^2\text{H}_{\text{alkane}}$) were unaffected by *n*-alkanes derived from background sources.

In order to determine if changes in $\delta^2\text{H}_{\text{alkane}}$ values are a function of the initial $^2\text{H}/^1\text{H}$ ratio of the solution ($\delta^2\text{H}_{\text{H}_2\text{O}}$), two experiments were conducted with similar temperatures, pressures and dissolved *n*-alkane concentrations but initial $\delta^2\text{H}_{\text{H}_2\text{O}}$ values both higher and lower than the starting $\delta^2\text{H}_{\text{alkane}}$ values, respectively. A temperature and pressure of 323°C and 35–36 MPa were

chosen for the experiments, respectively, in line with previous experiments conducted at 300–350°C and 35MPa where alkane-alkene equilibrium was demonstrated (Seewald, 1994, 2001a). This temperature is consistent with conditions in many ridge-crest hydrothermal fluids, but is higher than the maximum temperatures typically associated with the production of thermogenic natural gas in slowly subsiding sedimentary basins (~150–230°C, Killips and Killips, 2005). However, some deeply buried gas accumulations can approach 250–300°C (Burruss and Laughrey, 2010), and it is possible that the alkane-alkene reactions presented here may indeed proceed at temperatures below 300°C. Experiment 1 (113 days duration) was conducted with an initial $\delta^2\text{H}_{\text{H}_2\text{O}}$ value of +507‰, whereas Experiment 2 (226 days duration) had an initial $\delta^2\text{H}_{\text{H}_2\text{O}}$ value of -802‰ during Stage 1. After 226 days in Experiment 2, the reversibility of $^2\text{H}/^1\text{H}$ transfer between water and dissolved *n*-alkanes was confirmed during Stage 2 (113 days duration) by injecting 15.0g of a ^2H -spiked fluid (containing 10mmol/kg NaCl) into the reaction cell, thereby raising the $\delta^2\text{H}_{\text{H}_2\text{O}}$ value of the fluid to +352‰. This had the effect of diluting the abundances of dissolved hydrocarbons by a factor of ~2. The injected fluid was not purged of O_2 with Ar gas prior to injection.

2.2 Analytical Methods

Concentrations of dissolved species were monitored as a function of time during each experiment by removing fluid aliquots (typically <1g each) into glass/PTFE gas-tight syringes. Prior to each sampling event, an initial aliquot (<1g) was withdrawn to flush the capillary exit tube and discarded.

Concentrations of total dissolved inorganic carbon (ΣCO_2) and hydrocarbons (C_1 to C_5 *n*-alkanes, methylpropane (*iso*-butane) and C_2 to C_5 *n*-alkenes) were determined using purge and trap gas chromatography. Fluid aliquots were injected into a sparge cell containing ~1mL of 25wt.% phosphoric acid to ensure quantitative extraction of aqueous ΣCO_2 . The evolved gases were cryofocussed on an *n*-octane-coated silica trap before direct transfer to a gas chromatograph

(GC) equipped with PorapakTM Q column and serially connected thermal conductivity and flame ionization detectors. Commercially available hydrocarbon and CO₂ gas standards were similarly cryofocussed and transferred to the GC column for calibration. In the case of homologues with multiple alkene isomers (C₄ and C₅), chromatographic separation and quantitation of the individual *n*-alkene isomers was not possible and reported concentrations reflect the sum of all alkene isomers (denoted as ΣC_n alkenes) eluting at the retention time of the corresponding terminal *n*-alkene standard. Furthermore, due to the co-elution of large methylpropane and *n*-butane peaks before and after comparatively small ΣC₄ alkene peaks, large integration errors are associated with concentrations of the latter. Accordingly, although the presence of C₄ alkenes was observed, total concentrations are not reported. Analytical uncertainties (2s) are ±5% for C₁ to C₅ *n*-alkanes and ΣCO₂ concentrations, and ±10% for alkenes and methylpropane concentrations.

Aqueous H₂ concentrations were determined by gas chromatography on a 5Å molecular sieve column using thermal conductivity detection and N₂ carrier gas after headspace extraction of dissolved gases (analytical error (2s) ±10%). Total dissolved sulfide (ΣH₂S) was determined gravimetrically for a single fluid sample at 218.8 days in Experiment 2, following acidification of the aliquot with a 25wt.% phosphoric acid solution and precipitation of evolved H₂S gas as Ag₂S in a 5wt.% AgNO₃ solution. The pH (at 25°C) of a single fluid sample at 287.9 days in Experiment 2 was measured using an Ag/AgCl combination reference electrode. Concentrations of Cl and any dissolved C₁ to C₅ *n*-alkanoic (carboxylic) acids formed were determined by ion chromatography on a Dionex DX500 system with conductivity detection using an IonPac[®] AS15 ion exchange and IonPac[®] ICE-AS1 ion exclusion column, respectively. Analytical uncertainties (2s) are ±5% for Cl and ±10% for *n*-alkanoic acids.

Fluid aliquots (1-2g) for isotope analyses of dissolved hydrocarbons were collected in glass gas-tight syringes and immediately transferred into evacuated glass serum vials with butyl rubber stoppers (BellCo Glass) until analyzed. To minimize contamination of samples by

background levels of hydrocarbons present in butyl rubber, the stoppers were boiled in 2N NaOH for 2–4hrs followed by rinsing and overnight immersion in Milli-Q water (Oremland et al., 1987). Previous experience has shown that despite boiling in NaOH, trace residual contaminants (mainly C₃ and C₄ compounds) are still released from the butyl rubber on the order of 10⁻⁸ mol C per stoppered serum vial. However, such contamination is still over 2 orders of magnitude lower than the amount of C present as added *n*-alkanes in each sample. $\delta^2\text{H}_{\text{alkane}}$ values for methane, ethane, propane, *n*-butane and *n*-pentane were determined by continuous flow Gas Chromatography/Pyrolysis/Isotope-Ratio Mass Spectrometry (GC/P/IRMS) on a Finnigan Delta^{Plus}XL mass spectrometer interfaced to an Agilent 6890 GC through a GCCIII interface. Fixed volume (loop) aliquots of the serum vial headspace were introduced to the GC/P/IRMS via a valve interfaced with the GC carrier flow. The pyrolysis furnace was held at 1440°C for quantitative conversion of carbon-bound H to H₂. Peaks of an organic working standard gas (propane, $\delta^2\text{H}_{\text{alkane}} = -150\text{‰}$, externally calibrated against V-SMOW and SLAP) were periodically introduced into chromatograms downstream of the analytical (Alltech AT-Q) column for pyrolytic conversion as per analyte peaks prior to entry into the IRMS ion source. Mass-2 and -3 signals were processed using the ISODAT software package (ThermoElectron) and corrected for the H₃⁺ factor (<5 ppm/mV) daily (Sessions, 2006). Whereas the pooled standard deviation (2s) of all hydrocarbon $\delta^2\text{H}$ analyses is less than $\pm 6\text{‰}$, it is difficult to estimate the overall accuracy of our analyses given that the range of $\delta^2\text{H}$ values reported here (-489‰ to +114‰) is beyond that of any available low molecular weight *n*-alkane $\delta^2\text{H}$ standards. Although we performed daily corrections for H₃⁺ production (an important source of bias), other effects of ‘scale compression’ (Coplen, 1988) are possible for the extreme compositions encountered during our experiments. Another potential source of inaccuracy in GC/P/IRMS analyses is a ‘memory effect’, whereby a peak in a given chromatogram may be influenced by a preceding adjacent peak which differs in $\delta^2\text{H}$ by several hundred per mil due to uncharacterized GC (*i.e.* column) and/or surface adsorption processes during pyrolytic conversion in the furnace (Wang and Sessions, 2008). For lipid $\delta^2\text{H}$

analyses, offsets of 2–4‰ of the per mil difference between adjacent GC peaks are possible (Wang and Sessions, 2008). Although the magnitude of effects on low molecular weight *n*-alkane $\delta^2\text{H}$ analyses are unknown, a bias of similar extent is unlikely to have affected methane, ethane, *n*-butane or *n*-pentane to an extent greater than the analytical uncertainty ($\pm 6\%$, 2s) because peaks of the preceding carbon number were less than 100‰ different in our samples. For our samples, offsets will be greatest for *n*-propane due to the large ($>100\%$) differences between *n*-propane and preceding ethane in some cases. Introduction of reference propane standard peaks of constant composition (-150%) between ethane and propane analyte peaks within chromatograms from both experiments indicated that any variability for samples with the most extreme isotopic compositions due to pyrolytic conversion ‘memory effects’ (approximately $+2.5\%$) was less than the typical analytical uncertainty.

The hydrogen isotope composition of water in experimental solutions ($\delta^2\text{H}_{\text{H}_2\text{O}}$) was determined using high-resolution laser absorption spectroscopy on a DLT-100 Liquid Water Isotope Analyzer at the California Institute of Technology according to the method of Wang et al. (2009b). Precisions were less than $\pm 4\%$ (2s) for all analyses. Independent analysis of the ^2H -enriched starting solution for Experiment 1 by conventional dual-inlet isotope-ratio mass spectrometry (Isotech Laboratories, Inc.) indicated a $\delta^2\text{H}_{\text{H}_2\text{O}}$ value of $+501 \pm 5\%$, which is consistent with the value obtained by laser absorption spectroscopy ($507 \pm 4\%$).

All $\delta^2\text{H}$ values are expressed relative to the Vienna Standard Mean Ocean Water (V-SMOW) scale by the relation:

$$\delta^2\text{H} = [\text{R}_{\text{MEAS}} / \text{R}_{\text{VSMOW}}] - 1 \quad (5)$$

where $\text{R} = ^2\text{H}/^1\text{H}$, MEAS refers the measured isotope ratio for a given bulk molecule and R_{VSMOW} is 155.76×10^{-6} (Hagemann et al., 1970). The per mil (‰) symbol used with $\delta^2\text{H}$ values implies a factor of 10^3 which is omitted from Eq. (5).

3. RESULTS

3.1 $^2\text{H}/^1\text{H}$ ratios

Based on H mass balance considerations, H exchange between aqueous hydrocarbons and water was not a viable mechanism to alter the isotopic composition of the water to detectable levels during the experiments. This was confirmed during both stages of Experiment 2 by measurements of the initial (-802‰ and +352‰) and final (-798‰ and +354‰) $\delta^2\text{H}_{\text{H}_2\text{O}}$ values (Table 1). Although the $\delta^2\text{H}_{\text{H}_2\text{O}}$ value was not determined at the end of Experiment 1, it is assumed that it did not vary during the course of the experiment from the initial value (+507‰), as was observed for Experiment 2.

Although it is likely that trace amounts of hydrocarbons were released from the mineral assemblage or starting solutions during our experiments, the similarity of initial C_1 and C_2 $\delta^2\text{H}_{\text{alkane}}$ values (Table 1) with the measured starting (time zero) compositions suggests that the effects of such contamination on alkane $\delta^2\text{H}$ variations were minimal. In previous experimental studies, the contaminants were dominated by methane and ethane whose release was limited to the initial heating stages (Seewald, 2001a). Furthermore, formation of trace amounts of hydrocarbons through mineral-catalyzed (Fischer-Tropsch-type) or aqueous reduction of CO_2 with H_2 (Seewald et al., 2006; McCollom and Seewald, 2007) can be excluded. Thermodynamic drives (i.e. $\Delta_r G$ at T, P) for the synthesis of dissolved C_1 to C_5 alkanes by such processes are strongly unfavorable ($\gg +25\text{kJ/mol}$) throughout both experiments.

Changes in the H isotopic composition of C_1 to C_5 *n*-alkanes were characterized by large variations in both rate and direction during the experiments (Figure 2). Firstly, for all homologues $\delta^2\text{H}_{\text{alkane}}$ values migrated toward the $\delta^2\text{H}_{\text{H}_2\text{O}}$ value in each experiment. By the end of Experiment 1, $\delta^2\text{H}$ values of all *n*-alkanes had increased to varying degrees from initial values that were lower than that of the solution, while in Stage 1 of Experiment 2, where initial *n*-alkane $\delta^2\text{H}$ values were initially much higher than that of the solution, all $\delta^2\text{H}_{\text{alkane}}$ values decreased to varying degrees. Except for CH_4 the trend of decreasing $\delta^2\text{H}_{\text{alkane}}$ values was reversed in Stage 2

of Experiment 2 following injection of $^2\text{H}_2\text{O}$ -spiked water that raised the $\delta^2\text{H}$ value of the reaction cell water above that of the *n*-alkanes (Figure 2). Secondly, changes in $\delta^2\text{H}_{\text{alkane}}$ values were consistently faster and larger for the C_3 to C_5 *n*-alkanes relative to ethane and methane in both experiments (Figure 2). Methane $\delta^2\text{H}$ values varied least in both experiments with only small increases and decreases (<30‰) evident, although in all cases the direction conformed to the higher homologues (Figure 2). Regardless of the $\delta^2\text{H}_{\text{H}_2\text{O}}$ value in both experiments, the rate of change in $\delta^2\text{H}_{\text{alkane}}$ values also consistently slowed with time for the C_3 to C_5 *n*-alkanes. Such decreases in the rate of change of $\delta^2\text{H}_{\text{alkane}}$ values were not discernable for methane and ethane on the timescales of the experiments. In addition, initial rates of $\delta^2\text{H}_{\text{alkane}}$ changes were consistently faster when the difference between the $\delta^2\text{H}_{\text{H}_2\text{O}}$ and initial $\delta^2\text{H}_{\text{alkane}}$ values ($\Delta^2\text{H}_{\text{H}_2\text{O-alkane}}$) was greater. An examination of the average rate of change in C_3 to C_5 $\delta^2\text{H}_{\text{alkane}}$ values over the first 100 days in each experimental stage indicates that changes were fastest in Stage 2 of Experiment 2 ($2.5 - 3.5 \text{ ‰ day}^{-1}$, $\Delta^2\text{H}_{\text{H}_2\text{O-alkane}}$ of 781 – 841‰) and were slowest in Experiment 1 ($1.2 - 1.9 \text{ ‰ day}^{-1}$, $\Delta^2\text{H}_{\text{H}_2\text{O-alkane}}$ of 601 – 643‰). Stage 1 of Experiment 2 had intermediate rates and $\Delta^2\text{H}_{\text{H}_2\text{O-alkane}}$ (2.1 – 2.7 ‰ day^{-1} , $\Delta^2\text{H}_{\text{H}_2\text{O-alkane}}$ of 667 – 709‰).

3.2 Dissolved species concentrations

3.2.1 H_2 and H_2S

Aqueous H_2 concentrations were between 0.26 to 0.65mmol/kg during both experiments (Table 2). Assuming activity coefficients of 1 for neutral species, the narrow range of dissolved H_2 activities ($a_{\text{H}_2(\text{aq})}$) in both Experiments 1 and 2 overlaps the $a_{\text{H}_2(\text{aq})}$ predicted by the triple point of the PPM mineral buffer (Figure 1). The effectiveness of the assemblage in buffering the fluid redox state is evident in the rapid rebound of $a_{\text{H}_2(\text{aq})}$ values after fluid injection in Experiment 2 (Table 2). The single $\Sigma\text{H}_2\text{S}$ measurement in Experiment 2 indicates that the PPM assemblage likely buffered the activity of $\text{H}_2\text{S}_{(\text{aq})}$ to near equilibrium values also (Figure 1), consistent with previous experimental observations (Seewald, 1994, 2001a; McCollom and Seewald, 2003b).

3.2.2 Hydrocarbons

With the exception of the initial sampling event in Experiment 1, and taking into account the dilution effects of H₂O injection in Experiment 2, the abundances of methane, ethane and propane showed little or no variation throughout both experiments (Figure 3). In Experiment 1, however, initial C₁ to C₅ *n*-alkane concentrations at 8.0 days were all ~25% lower than subsequent sampling events (Table 2). No such trend was observed in the Cl concentration over the same period and the same behavior was not observed in Experiment 2, suggesting calibration/operator error may have influenced measured concentrations on this sampling event. Following minor initial increases, small but gradual decreases in the concentrations of *n*-pentane and *n*-butane occurred in Experiment 1 and during both stages of Experiment 2 (Table 2). Maximum overall losses in any given stage were <55% for *n*-pentane and <20% for *n*-butane.

Concentrations of ethene (51 – 93 nmol/kg) and propene (0.26 – 1.0 μmol/kg) varied by less than a factor of 4 during both experiments (Table 2). ΣC₅ alkene concentrations (0.016 – 0.30 mmol/kg) initially increased with time during the first stage of Experiment 2 but did not vary substantially during the second stage or during Experiment 1. Gradual production of methylpropane (up to 0.13 mmol/kg) was observed in both experiments (Table 2).

3.2.3 ΣCO₂ and organic acids

Rapid increases in the concentrations of ΣCO₂ (0.85–1.4mmol/kg, Table 2) were observed in the initial stages of both experiments and most likely reflect thermocatalytic production of CO₂ from contaminant carbon in the PPM mineral assemblage (Seewald, 1994, 2001a; McCollom and Seewald, 2003b). During later stages of both experiments, however, ΣCO₂ continued to increase gradually (Figure 3). Excluding the first sampling events, mass balance calculations indicate that the total concentration of dissolved carbon species (C_T) was relatively invariant after the initial stages of both experiments (Table 1), precluding the mineral buffer as

the source of ΣCO_2 with time during the later stages. The gradual ΣCO_2 increases were accompanied by systematic decreases of C_4 and C_5 hydrocarbons (Table 2) suggesting hydrocarbon oxidation as the source of ΣCO_2 , consistent with observations from previous experiments (Seewald, 2001a).

Formation of ethanoic and propanoic acid was observed throughout both experiments reaching concentrations of 0.49 mmol/kg (Table 2). Propanoic acid, though identified, was not present in quantifiable concentrations ($>0.1\text{mmol/kg}$) except in the later part of Stage 1 of Experiment 2. As is the case for ΣCO_2 , organic acids are produced during *n*-alkane oxidation and exclusive formation of C_2 and C_3 *n*-alkanoic acids is consistent with the decomposition of C_4 and C_5 *n*-alkanes (Seewald, 2001b). After injection of H_2O in Experiment 2 (Table 2), the concentration of ethanoic acid decreased by $<20\%$ which is smaller than expected for the estimated dilution factor of 2.1 due to fluid addition. In addition, decreases in *n*-pentane and *n*-butane (both $\sim 70\%$) after dilution were greater than expected. Although the excess carbon present as ethanoic acid relative to that predicted by dilution ($\sim 0.4\text{ mmol C/kg}$) is less than the carbon lost from the C_4 and C_5 alkanes after dilution ($\sim 1.2\text{ mmol C/kg}$), it does suggest that some oxidation of the latter may have occurred upon injection of O_2 -equilibrated H_2O spiked with $^1\text{H}_2\text{O}$. Despite these losses, significant changes in $\delta^2\text{H}$ values for *n*-butane and *n*-pentane were not evident (Figure 2), indicating that any decomposition had a minimal isotopic effect relative to the large variations in $\delta^2\text{H}$ values observed for these compounds.

4. DISCUSSION

4.1 Alkane-alkene equilibrium and reversible $^2\text{H}/^1\text{H}$ exchange

Experiments 1 and 2 demonstrate that reversible reaction of *n*-alkanes and their corresponding alkenes in conjunction with water disproportionation (reactions (1) and (4)) represents an indirect mechanism for $^2\text{H}/^1\text{H}$ exchange between water and C_{2+} *n*-alkanes under hydrothermal conditions. Hydrogen exchange is an unavoidable consequence of this process due to the reversible addition and removal of water-derived H_2 . Although alkene hydrogenation may not necessarily occur by direct addition of aqueous H_2 to double bonds, and other, more complex mechanisms may be involved, water is clearly the ultimate source of exchangeable H – as demonstrated by equilibrium according to reactions (2) to (4), (Figure 1). A lack of substantial H exchange in methane (which lacks a C_1 alkene), and the attainment of metastable thermodynamic equilibrium between several higher *n*-alkanes, their corresponding terminal *n*-alkenes and H_2 in both experiments (reaction (1)) both support this. The latter can be demonstrated by calculating the expected alkene concentrations at thermodynamic equilibrium. Using equilibrium constants for reaction (1) and - assuming unit activity coefficients for neutral species - measured concentrations of respective *n*-alkanes and H_2 , calculated metastable equilibrium abundances of ethene and propene according to reaction (1) are consistent with measured values throughout the experiments (Figure 4). Rapid equilibration of C_4 and C_5 *n*-alkanes and their corresponding *n*-alkenes is also likely to have occurred, but cannot be assessed due to the lack of concentration data for individual alkene isomers during the experiment and thermodynamic data for non-terminal *n*-alkenes. Numerous studies have shown that terminal alkene double bonds can migrate internally in aqueous aliphatic hydrocarbons at elevated temperatures and pressures (Hoering, 1984; Weres et al., 1988; Siskin et al., 1990; Leif and Simoneit, 1995, 2000; Seewald, 2001a, 2001b) and it is likely that this process occurred during both experiments. ΣC_5 *n*-alkene concentrations remain relatively constant or gradually increase with time in both experiments, and are greater than predicted equilibrium values for 1-pentene, suggesting that numerous C_5 *n*-

alkene isomers were present and possibly attained metastable thermodynamic equilibrium with *n*-pentane.

Although the attainment of alkane-alkene equilibria during the experiments provided a pathway for $^2\text{H}/^1\text{H}$ exchange, catalytic effects may have enhanced exchange rates. Seewald (2001a) demonstrated that alkane-alkene equilibration occurred faster in the presence of sulfur-bearing mineral assemblages relative to sulfur-free experiments buffered at the same redox state. They attributed this difference to the presence of aqueous sulfur species derived from the mineral buffer (Seewald, 2001a). The reactions nonetheless proceeded to equilibrium on a relatively rapid timescale in the absence of sulfur. In addition to the aqueous inorganic S-species postulated by Seewald (2001a), it is possible that alkyl thiol ($\text{C}_n\text{H}_{2n+1}\text{SH}$) compounds serve as intermediate species that facilitate rapid interconversion of alkenes to alkanes and vice versa. For example, H_2S may be particularly reactive toward alkene double bonds at elevated temperatures, thereby forming alkyl thiols that may then decompose to form alkanes (Ho et al., 1974; Krein, 1993; Martin, 1993; Zhang et al., 2008). Overall exchange must nonetheless occur via alkane-alkene equilibrium and, as stated previously, such reactions proceed readily in the absence of sulfur.

According to Sessions et al. (2004), mechanisms by which $^2\text{H}/^1\text{H}$ ratios in organic molecules are altered by exogenous H incorporation can be classified into five general categories. These consist of ‘pure exchange’ (where reactants and products are isotopically different but structurally and chemically identical), ‘stereochemical exchange’ (isotopic substitutions related to chiral inversions), ‘constitutional exchange’ (where reactants and products are constitutional isomers), and net transfer mechanisms such as ‘addition’ and ‘loss’ in which a reaction leads to a net transfer of H to or from the molecule. When viewed in isolation, the conversion of *n*-alkanes to *n*-alkenes technically implies an H ‘loss’ reaction (and the reverse ‘addition’) in the above classification. However, the requisite $\text{H}_{2(\text{aq})}$ for alkene hydrogenation is ultimately provided by the disproportionation of water (reaction (4)) and both reactions (1) and (4) are rapid and reversible at elevated temperatures (Seewald, 1994, 2001a). Hence, though the actual $^2\text{H}/^1\text{H}$

exchange takes place indirectly by a sequence of ‘loss’ and subsequent ‘addition’ transfer mechanisms (and probably ‘constitutional’ isomerization between these steps), when coupled together the overall reversible H transfer between water and *n*-alkanes is analogous to a ‘pure exchange’ mechanism. H transfer to and from *n*-alkanes is facilitated by the sluggish nature of overall stepwise oxidation reactions at the redox state employed, as demonstrated by the persistence of *n*-alkanes in solution. The oxidative losses (in excess of dilution) of *n*-butane and *n*-pentane observed upon injection of H₂O in Experiment 2 produced no noticeable change in $\delta^2\text{H}_{\text{alkane}}$ values for these homologues (Figure 2), suggesting that any inherent kinetic isotope effects are small relative to the large shifts produced by alkane-alkene equilibrium.

4.1.1 Alkene isomerization and abundance effects on $\delta^2\text{H}_{\text{alkane}}$ trends

A key observation from the experiments is the substantially faster and larger isotopic shifts for the C₃₊ hydrocarbons relative to ethane (Figure 2). This may be partly the result of exchange rate enhancements by ‘constitutional exchange’ during isomerization of C₃₊ *n*-alkenes prior to hydrogenation back to their corresponding *n*-alkanes. The absence of ethene isomerization limits hydrogen exchange to reversible oxidation-reduction and therefore slower rates of exchange. As stated previously, it is widely acknowledged that terminal double bonds in aliphatic alkenes can rapidly migrate (*i.e.* isomerize) to internal positions under acidic conditions at elevated temperatures. Seewald (2001a) observed rapid isomerization of 1-butene to all possible *n*-butene isomers on timescales of hours at 300°C under PPM-buffered conditions and extensive double bond migration has also been observed during hydrous pyrolysis of C₁₀, C₁₄ and C₁₆ terminal alkenes, leading to substantial ²H incorporation when pure ²H₂O was used (Hoering, 1984; Weres et al., 1988; Siskin et al., 1990; Leif and Simoneit, 1995, 2000). Hydrogenation of internal double bonds would contribute to ²H/¹H exchange on internal C–H bonds in *n*-alkanes. The possibility of both isomerization within individual alkenes and reversible *n*-alkane

equilibrium with multiple alkene isomers implies that all H positions in an individual n -alkane are exchangeable within the overall framework of reaction (1), (Figure 5).

While isomerization processes are undoubtedly a factor, additional influences such as the absolute abundance of n -alkenes could also contribute to more rapid exchange in higher n -alkanes relative to ethane. The rate at which isotopic exchange occurs will depend in part on the abundance of alkene species according to reaction (1). Thermodynamic data for reaction (1) indicates that C_{3+} n -alkenes are substantially more stable than ethene at equilibrium (Figure 6), consistent with measured concentrations during the experiments (Figure 4). Based on the data in this study, it is not possible to assess the relative influences of isomerization and alkene abundances on increased observed exchange rates relative to ethane.

4.1.2 Isotopic equilibrium effects on δ^2H_{alkane} trends

During both experiments, the rate of hydrogen isotopic exchange in the C_3 to C_5 n -alkanes decreased with time in both experiments (Figure 2). Such trends are identical to those observed in non-labile kerogen H during hydrous pyrolysis with waters of differing δ^2H values (Schimmelmann et al., 1999). Although steady state δ^2H values were not achieved in our experiments, which would be consistent with isotopic equilibrium, the above rate behavior combined with the directionality of variations strongly suggests that isotope equilibrium was being approached between the C_{2+} n -alkanes and water. This is consistent with the reversible and linked nature of the alkane-alkene and water disproportionation reactions. When a reservoir of H (alkane H) is approaching isotopic equilibrium with another reservoir that is vastly in excess (*i.e.* water H), the rate of change of $^2H/^1H$ ratios tends to follow pseudo first-order kinetics according to the following equation (Sessions et al., 2004):

$$\frac{F_t - F_{eq}}{F_i - F_{eq}} = e^{-kt} \quad (6)$$

Where F is the fractional abundance of ^2H ($= ^2\text{H}/(^2\text{H} + ^1\text{H})$) in the organic molecule initially, at time t , and at equilibrium, and k refers to the rate constant of exchange. The equilibrium isotope fractionation factor can be derived from F_{eq} ($= R_{eq}/(1 + R_{eq})$) and the $\delta^2\text{H}_{\text{H}_2\text{O}}$ value. For n -alkanes, both the F_{eq} and k terms in the strictest sense will depend on the nature of carbon-bound H in question (*i.e.* terminal methyl or internal methylene-bound H) and although equation (6) is exact for methane and ethane, more complex mathematical forms considering F_{eq} and k values specific to individual H positions are required to accurately model exchange in larger hydrocarbons (Sessions et al., 2004). However, the bulk H in n -alkanes will follow the general asymptotic form of equation (6), resulting in decreasing $\delta^2\text{H}_{\text{alkane}}$ changes in the bulk molecule per unit time. Observed exchange rates will also vary depending on how far the bulk $\delta^2\text{H}$ value is from the equilibrium state. Though equilibrium isotope fractionation factors would be equivalent in both Experiments 1 and 2 regardless of the water $\delta^2\text{H}$ values, isotopic shifts were faster when the $\delta^2\text{H}_{\text{alkane}}$ values were farthest from those of the solution, and presumably equilibrium.

Significant advances have been made in theoretical predictions of equilibrium isotope fractionation factors ($\alpha_{o/w}$) between organically-bound (o) and liquid water (w) hydrogen at low temperatures (Knyazev, 1992; Sessions et al., 2004; Schimmelmann et al., 2006; Wang et al., 2009b, 2009c):

$$\alpha_{o/w} = \frac{R_o}{R_w} = \frac{\delta^2H_o + 1}{\delta^2H_w + 1} \quad (7)$$

As numerical errors can be introduced by interconverting hydrogen isotope $\alpha_{o/w}$ values with per mil differences (ϵ values) between $\delta^2\text{H}_{\text{H}_2\text{O}}$ and $\delta^2\text{H}_{\text{alkane}}$ values (Sessions and Hayes, 2005), only the exact expression (7) is used here to describe fractionations. Little is known about the magnitude of $\alpha_{o/w}$ values for C_{2+} n -alkanes at higher temperature conditions typical of hydrothermal systems and natural gas deposits. Recent experimentally calibrated theoretical estimates of $\alpha_{o/w}$ for C_2 to C_5 n -alkanes between 0 and 100°C (0.845 to 0.896) indicate that $\delta^2\text{H}_{\text{alkane}}$ values should be more than 100‰ lower than 0‰ water at isotopic equilibrium (Wang et

al., 2009b, 2009c). Fractionation factors for the C₃₊ *n*-alkanes show only minor temperature dependence (< ~10‰) over the 100°C calibrated range and decreasing chain length dependence with temperature (Wang et al., 2009c). Although isotopic equilibrium was not attained in either of the experiments, minimum estimates of $\alpha_{o/w}$ can at least be calculated using Equation (7) for propane, *n*-butane and *n*-pentane based on the final fluid samples. Minimum estimated $\alpha_{o/w}$ values are 0.673, 0.708 and 0.739, respectively, for propane, *n*-butane and *n*-pentane in Experiment 1 where differences between water and hydrocarbon $\delta^2\text{H}$ values were smallest. It is important to recognize, however, that the actual equilibrium $\alpha_{o/w}$ values could be much higher had the experiment continued. Given the comparatively sluggish changes in ethane and methane $\delta^2\text{H}$ values, these calculations do not provide useful estimates of $\alpha_{o/w}$ values for these compounds.

4.1.3 Variations in $\delta^2\text{H}_{\text{methane}}$

Despite the inability of reaction (1) to allow isotopic exchange for methane, minor shifts (<30‰) were observed in $\delta^2\text{H}_{\text{methane}}$ values that followed the direction of the higher hydrocarbons in each experiment. While it is possible that these trends reflect sluggish exchange of methane H by an alternative mechanism, such as H abstraction and replacement, additions of CH₄ from degradation of isotopically exchanged C₄–C₅ *n*-alkanes or other sources must also be considered. For example, production of minor amounts of isotopically labeled methane by pyrolysis of carbon contaminants in the mineral buffer could have occurred. However, contaminant methane does not appear to have shifted measured $\delta^2\text{H}_{\text{methane}}$ values relative to initial compositions in the early stages of the experiments, when the majority of such methane would likely have been released from minerals (Seewald, 2001a). The minor decrease in $\delta^2\text{H}_{\text{methane}}$ and $\delta^2\text{H}_{\text{ethane}}$ following injection of water in Experiment 2 is of similar magnitude and could reflect addition of minor amounts of methane and ethane from degradation of the added longer chain alkanes as observed in previous experiments (Seewald, 2001a). Methane concentrations remained constant during both experiments except for the initial sample in Experiment 1 (Figure 3). Hence, in the absence of

exchange, methane contributions within analytical uncertainty from degrading higher alkanes are required to explain the observed long-term isotopic shifts. Isotope mass balance indicates that to produce the +28‰ shift in $\delta^2\text{H}_{\text{meth}}$ values (Experiment 1) requires added CH_4 to have a $\delta^2\text{H}$ value of approximately +380‰. Similar calculations for Stage 1 of Experiment 2 require addition of methane with $\delta^2\text{H}_{\text{methane}}$ values of approximately -600‰. In both instances production of methyl groups with extreme $^2\text{H}/^1\text{H}$ ratios near that of either the ambient water or heavily exchanged alkanes is required for such degradation to be considered a possible source. Changes in $\delta^2\text{H}_{\text{methane}}$ were also in the later stages of the experiments when some degradation had occurred. We therefore cannot completely exclude such contributions as a possible cause of $\delta^2\text{H}_{\text{methane}}$ variability. However, this implies that the ‘capping’ hydrogen involved in quenching methyl radicals formed during degradation also had similar $\delta^2\text{H}$ values to the precursor alkanes undergoing degradation or the water involved. This seems unlikely given that aqueous H_2 , for example, is typically extremely depleted in ^2H relative to the water from which it forms (Sherwood Lollar et al., 1993b, 2002; Proskurowski et al., 2006, 2008; Fu et al., 2007). Minor exchange of H by some sluggish mechanism may therefore provide a simpler explanation for the slow changes in $\delta^2\text{H}_{\text{methane}}$ values.

4.2 Implications for natural systems

4.2.1 $^2\text{H}/^1\text{H}$ ratios and abiogenesis in igneous environments

The abiogenic formation of aliphatic hydrocarbons during hydrothermal alteration of ultramafic crust has been extensively discussed (Abrajano et al., 1988, 1990; Sherwood et al., 1988; Charlou et al., 2002; Proskurowski et al., 2006, 2008; McCollom and Seewald, 2007; Konn et al., 2009). Though the exact mechanism for production of *n*-alkanes in highly-reducing crustal fluids is uncertain, it is assumed to be analogous to the industrial Fischer-Tropsch reaction and involves both reduction of inorganic carbon (CO_2 or CO) to methyl/methylene moieties and subsequent polymerization on a catalytic mineral surface (see review in McCollom and Seewald,

2007). In an effort to gain further insight into this phenomenon, measurements of $^2\text{H}/^1\text{H}$ ratios have recently been performed in addition to stable carbon isotope ratios (Sherwood Lollar et al., 2002; Fu et al., 2007; Proskurowski et al., 2008; McCollom et al., 2010). Because of the larger relative mass difference between ^2H and ^1H , substantial kinetic H isotope fractionation could occur between homologues during abiogenic polymerization. Based on $\delta^2\text{H}$ values of putative abiogenic $\text{C}_1\text{--}\text{C}_4$ *n*-alkanes recovered from saline fracture waters in crystalline basement igneous rocks of the Canadian Shield, Sherwood Lollar et al. (2002) proposed a characteristic H isotope trend with carbon number whereby $\delta^2\text{H}_{\text{methane}}$ values typically below -400‰ are extremely low relative to the $\text{C}_2\text{--}\text{C}_4$ alkanes ($\delta^2\text{H}_{\text{alkane}} \sim -220$ to -320‰), which become enriched in ^2H with increasing carbon number (Figure 7). This trend with carbon number is widespread among gases from Precambrian Shield (Sherwood Lollar et al., 2002, 2006, 2008) and is postulated to reflect preferential cleavage of $^{12}\text{C}\text{--}^1\text{H}$ bonds relative to $^{12}\text{C}\text{--}^2\text{H}$ bonds during the abiogenic polymerization process. The extremely ^2H -depleted nature of these alkanes is thought to reflect synthesis from H_2 with very low $\delta^2\text{H}$ values (often below -600‰ , Sherwood Lollar et al. (1993b, 2002)). This would be consistent with limited experimental data on the $\delta^2\text{H}_{\text{alkane}}$ values of hydrocarbons produced during aqueous Fischer-Tropsch-type synthesis, which suggests that alkanes form with relatively minor kinetic H isotope fractionation relative to H_2 (Fu et al., 2007; McCollom et al., 2010). These depletions and trends with carbon number have not, however, been observed in purported abiogenic hydrocarbons from higher temperature settings (Figure 7), such as those present in vent fluids of the Lost City hydrothermal site (Proskurowski et al., 2008), thereby complicating the elucidation of hydrocarbon provenance there. Based on the experimental observations of reversible exchange presented here, this discrepancy may reflect partial or complete alkane-water H isotope exchange that overprints isotope signatures associated with abiotic synthesis.

Recent theoretical equilibrium fractionation factors for H exchange between C_{2+} alkanes and water (0 to 100°C , Wang et al., 2009b, 2009c), combined with existing data for methane-

water isotopic equilibrium (0 to 370°C, Horibe and Craig (1995)), permit an evaluation of alkane-water isotopic equilibrium for hydrocarbons dissolved in Precambrian Shield fracture waters and Lost City hydrothermal fluids, given that *in situ* temperatures are below ~100°C in both systems. Using published $\delta^2\text{H}_{\text{H}_2\text{O}}$ values for fracture waters and hydrothermal fluids, the form of equation (7) can be used to calculate ‘observed’ fractionations for the Canadian Shield (Kidd Creek Mine, Sherwood Lollar et al. (2002)) and Lost City *n*-alkanes (Proskurowski et al., 2008). Examination of Figure 8 reveals that the Kidd Creek Mine *n*-alkanes are extremely depleted in ^2H relative to theoretical predictions for isotopic equilibrium with water. Observed fractionations for other low temperature (<100°C) microbial/abiogenic low molecular weight *n*-alkanes from crystalline rock aquifers in the Witwatersrand Basin, S. Africa (Ward et al., 2004; Lin et al., 2006; Onstott et al., 2006; Sherwood Lollar et al., 2008) and Fennoscandian Shield (Nurmi et al., 1988; Sherwood Lollar et al., 1993a, 1993b) are also much lower than equilibrium predictions at the temperatures likely experienced by these systems. Although partial isotopic exchange cannot be discounted, isotopic equilibrium between water and alkane H at ~35–60°C (Sherwood Lollar et al., 2008) is not evident despite the long residence time (on the order of tens of Ma, Lippmann et al. (2003)) of dissolved gases within basement rock at these conditions. These data suggest that the alkane-alkene mechanism may not be able to effectively promote H exchange in C_{2+} hydrocarbons at such low temperatures, which is consistent with the drastic decrease in alkene stability according to reaction (1) with decreasing temperature (Figure 6) and the potential kinetic barriers for chemical equilibrium inherent at the low temperatures of these systems.

In contrast to the Precambrian shield gases, abiogenic C_1 to C_3 *n*-alkanes in vent fluids at Lost City (44–91°C, Figure 7) are much more ^2H -enriched ($\delta^2\text{H}$ of -119 to -171‰, Proskurowski et al. (2008)). This is at odds with the conceptual model of Sherwood Lollar et al. (1993b, 2002), which would predict more depleted values due to abiogenic formation from the extremely ^2H -depleted $\text{H}_{2(\text{aq})}$ there (-600 to -700‰, Proskurowski et al. (2006)). In addition, there is no strong trend of increasing $\delta^2\text{H}_{\text{alkane}}$ with carbon number. Although the considerable overlap with the

range of thermogenic values (Figure 7) tentatively suggests that the alkanes could be derived from pyrolysis of pre-existing organic matter, a more likely explanation is that partial or near-complete alkane-water exchange has overprinted any highly ^2H -depleted signatures and trends that may have resulted from abiogenesis. Indeed, observed fractionations for many of the Lost City hydrocarbons approach, and in some cases attain (e.g. ethane), values predicted for alkane-water equilibrium at *in situ* conditions (Figure 8). The likelihood of ethane-water isotopic equilibrium mediated by reaction (1) is further supported by the presence of ethene in these fluids at concentrations of 1–40nmol/kg (Proskurowski et al., 2008). Based on the endmember ethane and H_2 concentrations reported by Proskurowski et al. (2008), these ethene concentrations are in excess of values predicted for equilibrium with ethane at the measured vent temperatures ($\leq 91^\circ\text{C}$), requiring instead temperatures $>300^\circ\text{C}$. There is extensive evidence, however, to suggest that Lost City fluids have cooled conductively during upflow and are considerably hotter (in the vicinity of $\sim 250^\circ\text{C}$) at depth (Allen and Seyfried, 2004; Proskurowski et al., 2006; Foustoukos et al., 2008). This suggests that chemical equilibrium in the ethane-ethene reaction may record higher temperatures deeper in the hydrothermal reservoir, as has been observed in the Middle Valley hydrothermal system (Cruse and Seewald, 2006). This results in an apparent discrepancy between the ethane-water isotopic equilibrium at lower (vent) temperatures and lack of concomitant chemical ethane-ethene equilibrium. However, the temperature dependence of alkane $\alpha_{o/w}$ values, which show very little variation below 100°C (Figure 8), are presently unknown at temperatures $>100^\circ\text{C}$, and the possibility exists that the hydrogen isotope composition of *n*-alkanes at Lost City may record higher temperature conditions. Evidence that isotopic equilibration may be occurring at higher temperatures is provided by the $\delta^2\text{H}$ values of aqueous methane that yield temperatures for methane water isotopic equilibrium of $\sim 190\text{--}250^\circ\text{C}$ using the equilibrium fraction factors of Horibe and Craig (1995), consistent with other estimates of reaction zone temperatures at depth (Allen and Seyfried, 2004; Proskurowski et al., 2006; Foustoukos et al., 2008).

Results of the experiments suggest that, with increasing temperatures, alkane-alkene equilibria may promote H isotopic exchange and possibly attainment of equilibrium between abiogenic *n*-alkanes and water. In other ultramafic-hosted hydrothermal systems where abiogenic hydrocarbon formation has been proposed, such as Rainbow and Logatchev (Holm and Charlou, 2001; Charlou et al., 2002; Schmidt et al., 2007; Konn et al., 2009), reaction zone temperatures are considerably higher than Lost City. Maximum measured vent fluid temperatures at both of these locations are in excess of 350°C and reaction zone conditions are thought to be nearer 400°C (Allen and Seyfried, 2003; Seyfried et al., 2004; Seyfried et al., 2011). The experiments presented here suggest substantial H isotope exchange between the C₂₊ alkanes and water can occur on timescales of months to years at 323°C, and even greater rates of isotope exchange are likely at the higher temperatures of these systems due to the enhanced stability of alkenes according to reaction (1) (Figure 6). Given that estimates of crustal residence times for hydrothermal solutions based on radioisotope methods (Kadko, 1996; Kadko and Butterfield, 1998) and geophysical considerations (Fisher, 2003) are on the order of years, sufficient time for isotopic equilibrium may be provided during hydrothermal circulation. Though H isotope data are lacking for C₂₊ alkanes at sites other than Lost City, evidence for ethane-ethene and propane-propene equilibria at reaction zone conditions in the sedimented Middle Valley hydrothermal system (Cruse and Seewald, 2006) suggests that alkane-water exchange may be commonplace in hydrothermal fluids containing C₂₊ *n*-alkanes. Accordingly, δ²H values for aqueous *n*-alkanes may not be an effective tool for the identification of abiogenic hydrocarbons in hydrothermal systems.

4.2.2 ²H/¹H signatures in thermogenic hydrocarbons

A common feature of thermogenic natural gases reported to date is a gradual increase in δ²H values with increasing carbon number (Figure 7) and overall ²H-enrichment in the homologous series as a whole with increasing thermal maturity (Schoell, 1983; Barker and

Pollock, 1984; Whiticar et al., 1985; Sherwood Lollar et al., 2002; Edwards et al., 2007; Boreham et al., 2008; Liu et al., 2008; Wang et al., 2009a; Burruss and Laughrey, 2010). As is the case for the higher *n*-alkanes in petroleum, this has traditionally been viewed as a kinetic isotope effect associated with C–C bond cleavage, which favors reaction of ²H-depleted larger molecules in cracking reactions (Schimmelmann et al., 2004). C(²H¹H)–C(¹H₂) bonds are stronger - and therefore considered slower to react - than C(¹H₂)–C(¹H₂) bonds and quenching of generated alkyl radicals by ‘capping’ hydrogen is likely to favor incorporation of ¹H relative to ²H (Sackett, 1978; Schimmelmann et al., 2004; Wang et al., 2009a). Recently, Ni et al. (2011) used theoretical quantum chemistry calculations of kinetic H isotope fractionation effects due to thermal cracking to develop a thermal maturity model for natural gas H isotope compositions. Based on correlations of thermal maturities calculated from the H isotope model with those derived from a similar model developed for kinetic ¹³C/¹²C fractionation, they propose that H isotopes in C₁ to C₃ *n*-alkanes of natural gases reflect predominantly maturation-related kinetic isotope effects. However, as noted by Ni et al. (2011), there is a high degree of scatter in these correlations for several basin-wide datasets, and they speculate that the generally poor correlations for propane may reflect H exchange with water. The authors suggest that ethane H, which shows the strongest correlation, may be least affected by isotope exchange with water, but our experimental results suggest that ethane exchange may also be significant on a geological timescale.

In environments where hydrocarbon formation is occurring by thermogenic processes, the potential for alkene-mediated H exchange between low molecular weight *n*-alkanes and water will clearly depend on the availability of aqueous fluids, in addition to redox and temperature. Water is a ubiquitous feature in sedimentary basins and there is substantial evidence to suggest it plays an important role in both the thermal maturation of sedimentary organic matter and the migration of generated light (<C₅) hydrocarbons (Lewan et al., 1979; Tissot and Welte, 1984; Lewan, 1997; Seewald, 1997). The extent of exchange will also depend on the redox state of aqueous fluids in which hydrocarbons are dissolved due to the nature of the alkane-alkene

reaction. Under reducing conditions, lower alkene abundances may result in slower rates of H isotope exchange, while oxidizing conditions would favor exchange, provided complete oxidation of hydrocarbons to CO₂ does not occur (Seewald, 2001a). The temperature dependence of reaction kinetics and alkene stability relative to their corresponding alkanes will also influence the rate of isotopic exchange. Most light (<C₅) hydrocarbons typically form below ~230°C where alkene stability is expected to be orders of magnitude lower than experimental conditions for a given H₂ activity (Figure 6), and consequently exchange by the alkane-alkene mechanism might be expected to be slower at lower temperatures. However, thermal maturation and migration processes in petroleum-producing systems typically occur over long (Ma) geologic timescales, which may facilitate extensive isotopic exchange, the slower reaction rates, notwithstanding. Also, temperatures in some deeply buried reservoirs, such as those found in the Appalachian Basin, USA, can be much higher (up to ~300°C, Burruss and Laughrey, 2010) and therefore more favorable for alkene formation. Although relatively few published data exist, *n*-alkenes are typically considered trace components of natural gas relative to *n*-alkanes (Whiticar, 1990; Harbert et al., 2006). However, as demonstrated during the experiments, even trace alkene abundances (e.g. ethane and propene, Table 2) still allow for considerable ²H/¹H exchange.

The typical ²H depletions and trends with carbon number reported for thermogenic gases are, however, also consistent with isotopic equilibrium with water H. Taking the example of wet (C₂₊ rich) thermogenic gases from southwestern Ontario, C₂₊ alkanes there are depleted in ²H relative to average saline reservoir waters of this region yielding observed fractionations (according to Eq. (7)) of approximately 0.85 to 0.92 (Sherwood Lollar et al., 1994, 2002). These values are consistent with the range of equilibrium fractionation factors ($\alpha_{o/w}$ of 0.87–0.89) derived by Wang et al. (2009c) at 100°C, the upper limit of theoretical $\alpha_{o/w}$ estimates (Figure 8). As stated previously, however, we do not know equilibrium $\alpha_{o/w}$ values for alkane H up to 200°C - the likely temperatures of maturation for these gases (Sherwood Lollar et al., 1994). However, if $\alpha_{o/w}$ values remain reasonably invariant beyond 100°C to maturation temperatures, then the

isotopic compositions of these gases would be consistent with equilibrium exchange with water. For higher temperature (250–300°C) deeply buried thermogenic gases from the northern Appalachian Basin, where basinal brine $\delta^2\text{H}_{\text{H}_2\text{O}}$ values range from -30‰ to -40‰ (Burruss and Laughrey, 2010), observed fractionations for ethane and propane (0.83–0.91) also overlap the highest temperature $\alpha_{o/w}$ estimates. Furthermore, $\delta^2\text{H}_{\text{methane}}$ values from the latter setting are consistent with $\text{CH}_4\text{-H}_2\text{O}$ isotopic equilibrium (according to the data of Horibe and Craig (1995)) at the estimated temperatures at depth (Burruss and Laughrey, 2010).

The gradual increase in $\delta^2\text{H}_{\text{alkane}}$ of ~0–30‰ with each increase in carbon number that is typical of reported thermogenic gases (Sherwood Lollar et al., 2002; Edwards et al., 2007; Boreham et al., 2008; Liu et al., 2008; Wang et al., 2009a; Burruss and Laughrey, 2010) is also generally consistent with the predicted chain length dependency of alkane-water equilibrium H isotope effects. According to the data of Wang et al. (2009c), calculated $\alpha_{o/w}$ values for ethane/water (0.878), propane/water (0.886), *n*-butane/water (0.890) and *n*-pentane/water (0.895) equilibrium at 100°C increase systematically with chain length. If alkanes were in equilibrium with a typical basinal brine having a $\delta^2\text{H}_{\text{H}_2\text{O}}$ value of -50‰, increases in $\delta^2\text{H}_{\text{alkane}}$ with carbon number would be on the order of 5‰. Although the magnitude of these offsets increases at lower temperatures (cf. Figure 8), the relative enrichments do not. This chain length dependency is related to the inductive electron-donating (+I) effect of terminal methyl (-CH₃) groups on adjacent internal methylene (-CH₂-) positions which increases stiffness in C–H bonds of the latter, thereby favoring slightly greater degrees of ²H substitution (Hartshorn and Shiner, 1972; Wang et al., 2009c). With increasing chain lengths beyond *n*-pentane, this effect gradually decreases due to increasing quantities of internal methylene groups (with uniform $\alpha_{o/w}$ values) but it has the capability to produce strikingly similar trends to those observed in thermogenic low molecular weight hydrocarbons.

While hydrocarbons beyond C₅ were not examined in this investigation, experimental evidence suggests that alkane-alkene reactions could also mediate extensive H exchange in longer

chain alkanes. In a series of hydrous pyrolysis experiments using pure $^2\text{H}_2\text{O}$ at 330–350°C, Leif and Simoneit (2000) demonstrated extensive double bond migration and concomitant ^2H incorporation during reaction of the terminal alkenes 1,13-tetradecadiene ($\text{C}_{14}\text{H}_{26}$) and 1-hexadecene ($\text{C}_{16}\text{H}_{32}$) with immature organic-rich shale. These shorter experiments (<72h) were conducted without intentional redox buffering, but minor amounts of ^2H -labeled alkanes were observed to form by reduction of these probe molecules. This suggests that alkane-alkene reactions enabled H isotope exchange in C_{10} – C_{16} hydrocarbons in the presence of the highly reducing shale and its kerogen complement. It has become increasingly recognized in recent years that $\delta^2\text{H}$ values of bulk sedimentary organic matter and its individual hydrocarbon constituents initially increase during thermal maturation but approach a near constant offset of 80–110‰ below that of associated waters, even with further increases in thermal maturity (Schimmelmann et al., 1999, 2001, 2006). The estimation of compound specific fractionation factors between alkane H and water H lead Wang et al. (2009c) to conclude that this offset can best be explained by isotopic exchange toward equilibrium between these two H reservoirs. Whereas Schimmelmann et al. (1999, 2001) argued that this exchange likely takes place as a result of reactions largely limited to the maturation process (*e.g.* cracking, isomerization, rearrangement etc.), the alkane-alkene mediated exchange demonstrated here could occur subsequent to the main stage of oil formation and would also allow for comprehensive exchange of aliphatic H in hydrocarbons.

Further constraints are required to confirm that the composition of thermogenic low molecular weight hydrocarbons do indeed reflect isotopic equilibrium with associated waters. These include more detailed evaluations of the isotopic composition of individual thermogenic gas constituents and associated basinal waters in the context of their thermal history, in addition to better estimates of alkane-water fractionations at higher temperatures to constrain the temperature dependence of $\alpha_{o/w}$ values at temperatures >100°C. The proximity of some thermogenic gas isotopic compositions to equilibrium values, and the increased recognition of

exchange in higher molecular weight petroleum constituents, however, provide a compelling argument that the H isotopic composition of thermogenic hydrocarbons may be governed by equilibrium rather than kinetic isotope effects both during and subsequent to maturation processes. Because equilibrium isotope fractionation only varies as a function of temperature and to a lesser extent pressure, the hydrogen isotope composition of hydrocarbons may be of limited use as an indicator of kinetically-controlled thermal maturation processes that vary as a function of both time and temperature.

5. CONCLUSIONS

An experimental investigation of $^2\text{H}/^1\text{H}$ exchange between low molecular weight ($<C_5$) aqueous *n*-alkanes and water under hydrothermal conditions shows that transfer of H isotopes can be readily mediated by rapid reversible metastable equilibria between *n*-alkanes and their corresponding *n*-alkenes, coupled with the disproportionation of water, which ultimately provides requisite H for hydrogenation. Rates of exchange are sufficiently rapid that drastic changes in alkane $\delta^2\text{H}$ values occur on timescales of months to years at 323°C. Much faster rates of exchange are observed for longer chains alkanes due to factors such as higher equilibrium alkene abundances and internal isomerization of terminal *n*-alkenes prior to hydrogenation. The evidence for exchange in methane is equivocal, but if it does occur rates are substantially slower than the higher homologues and exchange would proceed on longer geological timescales.

Based on recent theoretical estimates of equilibrium fractionation between hydrocarbon H and water H, previously reported *n*-alkanes of putative abiogenic origin from low temperature Precambrian Shield basement are too depleted in ^2H relative to equilibrium fractionation effects and are thus unlikely to have experienced extensive exchange. Abiogenic hydrocarbons from the higher temperature Lost City hydrothermal field, in contrast, appear to have undergone exchange following synthesis at reaction zone conditions. The proximity of many of these hydrocarbon $^2\text{H}/^1\text{H}$ ratios to values predicted for isotopic equilibrium with water suggests that the observed disparity between these and the Canadian Shield hydrocarbons reflects exchange effects subsequent to abiogenesis. Though further confirmation is needed, the H isotopic composition of many thermogenic gases is also suggestive of isotopic equilibrium with water, rather than kinetic isotope effects related to thermal maturation. This is consistent with the emerging realization of extensive exchange in higher petroleum hydrocarbons that have experienced elevated temperatures.

Acknowledgements

The authors are very grateful to Prof. Alex Sessions for providing a thorough and insightful review of this manuscript. The authors also wish to thank Dr. Ying Wang and an anonymous reviewer for helpful and constructive reviews, and Associate Editor R. Burruss for editorial handling. This research received financial support from the Department of Energy (grant DE-FG02-97ER14746), the National Science Foundation (grant OCE-0549829) and the WHOI Deep Ocean Exploration Institute Graduate Fellowship (to E.P. Reeves). Financial support during editing of this manuscript was provided by the DFG Research Center/Cluster of Excellence MARUM “The Ocean in the Earth System”.

Figure Captions

Figure 1. Activity diagram showing the phase relations in the system Fe-S-O-H at 325°C and 35MPa. Requisite data for the construction of this figure were obtained from the SUPCRT92 database (Johnson et al., 1992). To account for the non-stoichiometric composition of pyrrhotite, requisite activities ($a_{\text{FeS(s)}}$) at conditions were calculated from the data of Toulmin and Barton (1964). The *gray square* denotes the activity of H₂S based on a single sample at 218.8 days in Experiment 2 and the associated *horizontal black line* denotes the range of aqueous H₂ activities observed during both Experiments 1 and 2. Activities of aqueous H₂S and H₂ were calculated assuming ideal behavior in solution.

Figure 2. $\delta^2\text{H}$ values for C₁ to C₅ *n*-alkanes from Experiment 1 (**a**) and Experiment 2 (**b**) as a function of time at 323°C and 35MPa. The vertical dashed line at 226 days in Experiment 2 represents injection of ²H-spiked water to raise the $\delta^2\text{H}_{\text{H}_2\text{O}}$ value of the solution in the reaction cell. The pooled standard deviation of all *n*-alkane $\delta^2\text{H}$ analyses ($\pm 6\%$, 2s) is smaller than the data symbols. Mean values of $\delta^2\text{H}_{\text{H}_2\text{O}}$ are annotated for each experimental stage. Concentrations of dissolved species were not monitored after 300 days in Experiment 2.

Figure 3. Concentrations of C₁ to C₅ *n*-alkanes and ΣCO_2 from Experiment 1 (**a**) and Experiment 2 (**b**) as a function of time at 323°C and 35MPa. The vertical dashed line at 226 days in Experiment 2 represents injection of ²H-spiked water, which diluted the reaction cell contents. Error bars represent 2s analytical uncertainties, which are smaller than the data symbols for propane, *n*-butane and *n*-pentane. Concentrations of dissolved species were not monitored after 300 days in Experiment 2.

Figure 4. Measured concentrations (solid lines) of C₂, C₃ and ΣC₅ *n*-alkenes in Experiment 1 (a) and Experiment 2 (b) as a function of time at 323°C and 35MPa. Predicted concentrations (dashed lines) are calculated using measured alkane and H₂ concentrations (assuming unit activity coefficients) and equilibrium constants for reaction (1). Requisite data for these calculations are taken from the SUPCRT92 database (Johnson et al., 1992) with additional data from Shock and Helgeson (1990). The vertical dashed line at 226 days in Experiment 2 represents injection of ²H-spiked water, which diluted the reaction cell contents. Concentrations of dissolved species were not monitored after 300 days in Experiment 2.

Figure 5. Proposed mechanism for the reversible equilibration of *n*-pentane with individual pentene isomers, in addition to internal isomerization reactions between C₅ *n*-alkenes. Asterisks denote the C positions where hydrogen may be exchanged during hydrogenation, dehydrogenation and isomerization. Similar mechanisms could be drawn for other *n*-alkanes with multiple potential alkene isomers.

Figure 6. Logarithm of the equilibrium constants (K_{eq}) for reactions between C₂ to C₅ *n*-alkenes and their corresponding terminal *n*-alkenes as a function of temperature at 35 MPa. For a given $a_{H_2(aq)}$, alkene/alkane activity ratios for the C₃₊ *n*-alkanes are over an order of magnitude higher than for ethane. Requisite data for the construction of this figure are taken from the SUPCRT92 database (Johnson et al., 1992) with additional data from Shock and Helgeson (1990).

Figure 7. Isotopograms showing the δ²H values of *n*-alkanes as a function of chain length from selected geological settings. Data for the putative abiogenic gases from Kidd Creek Mine (*black dots*, Sherwood Lollar et al. (2002)) and Lost City hydrothermal vent fluids (*open diamonds*, Proskurowski et al. (2008)) are shown, although δ²H values for *n*-butane were not reported for the latter setting. Ranges for a large selection of thermogenic gas data (*gray area*) reported from gas

fields in continental North America (Sherwood Lollar et al., 1994, 2002; Burruss and Laughrey, 2010; Ni et al., 2011), Australia (Edwards et al., 2007; Boreham et al., 2008; Ni et al., 2011), China and the Gulf of Thailand (Liu et al., 2008; Wang et al., 2009a; Ni et al., 2011) are plotted for comparison. The narrow range of plotted $\delta^2\text{H}_{\text{alkane}}$ values for thermogenic *n*-butane is due to such data only being reported for the Southwest Ontario (Sherwood Lollar et al., 1994, 2002) and Carnarvon Basin gases (Edwards et al., 2007; Boreham et al., 2008).

Figure 8. Plot of observed alkane-water H isotope fractionations (according to Equation (7)) for Kidd Creek Mine (*open symbols*, Sherwood Lollar et al. (2002)) and Lost City vent fluid (*gray symbols*, Proskurowski et al. (2008)) $\delta^2\text{H}_{\text{alkane}}$ values versus *in situ* temperatures. Also plotted (*lines*) are theoretical alkane-water equilibrium hydrogen isotope fractionation factors ($\alpha_{o/w}$) as a function of temperature for CH_4 (data from Horibe and Craig (1995)) and C_{2+} *n*-alkanes (data from Wang et al. (2009c)). For the Kidd Creek Mine gases, fracture waters are assumed to be relatively uniform temperature ($\sim 35^\circ\text{C}$, Sherwood Lollar et al. (2008)) and an average $\delta^2\text{H}_{\text{H}_2\text{O}}$ value of -71‰ is chosen based on the range (-68 to -74‰) reported by Sherwood et al. (1988). For Lost City, accompanying vent fluid temperatures (Proskurowski et al., 2008) are plotted and an average $\delta^2\text{H}_{\text{H}_2\text{O}}$ value of $+5\text{‰}$ is chosen based on the range ($+2$ to $+7\text{‰}$) reported by Proskurowski et al. (2006).

References

- Abrajano, T. A., Sturchio, N. C., Bohlke, J. K., Lyon, G. L., Poreda, R. J., and Stevens, C. M., (1988) Methane hydrogen gas seeps, Zambales Ophiolite, Philippines - deep or shallow origin. *Chemical Geology* **71**, 211-222.
- Abrajano, T. A., Sturchio, N. C., Kennedy, B. M., Lyon, G. L., Muehlenbachs, K., and Bohlke, J. K., (1990) Geochemistry of reduced gas related to serpentinization of the Zambales Ophiolite, Philippines. *Applied Geochemistry* **5**, 625-630.
- Allen, D. E. and Seyfried, W. E., (2003) Compositional controls on vent fluids from ultramafic-hosted hydrothermal systems at mid-ocean ridges: An experimental study at 400°C, 500 bars. *Geochimica et Cosmochimica Acta* **67**, 1531-1542.
- Allen, D. E. and Seyfried, W. E., (2004) Serpentinization and heat generation: Constraints from Lost City and Rainbow hydrothermal systems. *Geochimica et Cosmochimica Acta* **68**, 1347-1354.
- Aubourg, C. and Pozzi, J.-P., (2010) Toward a new <250°C pyrrhotite–magnetite geothermometer for claystones. *Earth and Planetary Science Letters* **294**, 47-57.
- Barker, J. F. and Pollock, S. J., (1984) The geochemistry and origin of natural gases in southern Ontario. *Bulletin of Canadian Petroleum Geology* **32**, 313-326.
- Bell, J. L. S., Palmer, D. A., Barnes, H. L., and Drummond, S. E., (1994) Thermal decomposition of acetate: III. Catalysis by mineral surfaces. *Geochimica et Cosmochimica Acta* **58**, 4155-4177.
- Berndt, M. E., Allen, D. E., and Seyfried, W. E., (1996) Reduction of CO₂ during serpentinization of olivine at 300 °C and 500 bar. *Geology* **24**, 351-354.
- Boreham, C. J., Edwards, D. S., Hope, J. M., Chen, J. H., and Hong, Z. H., (2008) Carbon and hydrogen isotopes of neo-pentane for biodegraded natural gas correlation. *Organic Geochemistry* **39**, 1483-1486.

- Burruss, R. C. and Laughrey, C. D., (2010) Carbon and hydrogen isotopic reversals in deep basin gas: Evidence for limits to the stability of hydrocarbons. *Organic Geochemistry* **41**, 1285-1296.
- Charlou, J. L., Donval, J. P., Fouquet, Y., Jean-Baptiste, P., and Holm, N., (2002) Geochemistry of high H₂ and CH₄ vent fluids issuing from ultramafic rocks at the Rainbow hydrothermal field (36°14'N, MAR). *Chemical Geology* **191**, 345-359.
- Coplen, T. B., (1988) Normalization of Oxygen and Hydrogen Isotope Data. *Chemical Geology* **72**, 293-297.
- Cruse, A. M. and Seewald, J. S., (2006) Geochemistry of low-molecular weight hydrocarbons in hydrothermal fluids from Middle Valley, northern Juan de Fuca Ridge. *Geochimica et Cosmochimica Acta* **70**, 2073-2092.
- Edwards, D. S., Boreham, C. J., Hope, J. M., Preston, J. C., Lepoidevin, S., Buckler, T., and Hong, Z., (2007) Molecular and stable isotope (D/H and ¹³C/¹²C) compositions of natural gas from the Exmouth Plateau and Rankin Platform, Carnarvon Basin, Australia. In: *The 23rd International Meeting on Organic Geochemistry, Torquay, England, 9th-14th September 2007. Book of Abstracts*, pp335-336.
- Eglinton, T. I. and Eglinton, G., (2008) Molecular proxies for paleoclimatology. *Earth and Planetary Science Letters* **275**, 1-16.
- Fisher, A. T., (2003) Geophysical constraints on hydrothermal circulation: observations and models. In: *Dahlem Workshop Report: Energy and Mass Transfer in Marine Hydrothermal Systems*, pp29-52. Halbach, P. E., Tunnicliffe, V., and Hein, J. R. (Ed.). Dahlem University Press.
- Foustoukos, D. I. and Seyfried, W. E., (2004) Hydrocarbons in hydrothermal vent fluids: The role of chromium-bearing catalysts. *Science* **304**, 1002-1005.

- Foustoukos, D. I., Savov, I. P., and Janecky, D. R., (2008) Chemical and isotopic constraints on water/rock interactions at the Lost City hydrothermal field, 30°N Mid-Atlantic Ridge. *Geochimica et Cosmochimica Acta* **72**, 5457-5474.
- Fu, Q., Sherwood Lollar, B., Horita, J., Lacrampe-Couloume, G., and Seyfried, W., (2007) Abiotic formation of hydrocarbons under hydrothermal conditions: Constraints from chemical and isotopic data. *Geochimica et Cosmochimica Acta* **71**, 1982-1998.
- Hagemann, R., Nief, G., and Roth, E., (1970) Absolute isotopic scale for deuterium analysis of natural waters: absolute D/H ratio for SMOW. *Tellus* **22**, 712-715.
- Harbert, W., Jones, V. T., Izzo, J., and Anderson, T. H., (2006) Analysis of light hydrocarbons in soil gases, Lost River region, West Virginia: Relation to stratigraphy and geological structures. *AAPG Bulletin* **90**, 715-734.
- Hartshorn, S. R. and Shiner, V. J., (1972) Calculation of H/D, $^{12}\text{C}/^{13}\text{C}$, and $^{12}\text{C}/^{14}\text{C}$ fractionation factors from valence force fields derived for a series of simple organic molecules. *Journal of the American Chemical Society* **94**, 9002-9012.
- Ho, T. Y., Rogers, M. A., Drushel, H. V., and Koons, C. B., (1974) Evolution of sulfur compounds in crude oils. *AAPG Bulletin* **58**, 2338-2348.
- Hoering, T. C., (1984) Thermal reactions of kerogen with added water, heavy water and pure organic substances. *Organic Geochemistry* **5**, 267-278.
- Holm, N. G. and Charlou, J. L., (2001) Initial indications of abiotic formation of hydrocarbons in the Rainbow ultramafic hydrothermal system, Mid-Atlantic Ridge. *Earth and Planetary Science Letters* **191**, 1-8.
- Horibe, Y. and Craig, H., (1995) D/H fractionation in the system methane-hydrogen-water. *Geochimica et Cosmochimica Acta* **59**, 5209-5217.
- Horita, J. and Berndt, M. E., (1999) Abiogenic methane formation and isotopic fractionation under hydrothermal conditions. *Science* **285**, 1055-1057.
- Hunt, J. M., (1996) *Petroleum Geochemistry and Geology*. 2nd Ed. W.H. Freeman and Company.

- Johnson, J. W., Oelkers, E. H., and Helgeson, H. C., (1992) SUPCRT92 - A software package for calculating the standard molal thermodynamic properties of minerals, gases, aqueous species, and reactions from 1 to 5000 bar and 0 to 1000°C. *Computers & Geosciences* **18**, 899-947.
- Kadko, D., (1996) Radioisotopic studies of submarine hydrothermal vents. *Rev. Geophys.* **34**, 349-366.
- Kadko, D. and Butterfield, D. A., (1998) The relationship of hydrothermal fluid composition and crustal residence time to maturity of vent fields on the Juan de Fuca Ridge. *Geochimica et Cosmochimica Acta* **62**, 1521-1533.
- Killops, S. and Killops, V., (2005) *An Introduction to Organic Geochemistry*. 2nd Ed. Blackwell Publishing.
- Knyazev, D. A., Myasoedov, N.F., Bocharov, A.V., (1992) The theory of the equilibrium isotope effects of hydrogen. *Russian Chemical Reviews* **61**, 204-220.
- Konn, C., Charlou, J. L., Donval, J. P., Holm, N. G., Dehairs, F., and Bouillon, S., (2009) Hydrocarbons and oxidized organic compounds in hydrothermal fluids from Rainbow and Lost City ultramafic-hosted vents. *Chemical Geology* **258**, 299-314.
- Krein, E. B., (1993) Organic sulfur in the geosphere: analysis, structures and chemical processes. In: *Supplement S: The chemistry of Sulphur-containing functional groups*, pp975-1032. Patai, S. and Rappoport, Z. (Ed.). Wiley.
- Leif, R. N. and Simoneit, B. R. T., (1995) Ketones in hydrothermal petroleums and sediment extracts from Guaymas Basin, Gulf of California. *Organic Geochemistry* **23**, 889-904.
- Leif, R. N. and Simoneit, B. R. T., (2000) The role of alkenes produced during hydrous pyrolysis of a shale. *Organic Geochemistry* **31**, 1189-1208.
- Lewan, M. D., Winters, J. C., and McDonald, J. H., (1979) Generation of oil-like pyrolyzates from organic-rich shales. *Science* **203**, 897-899.

- Lewan, M. D., (1997) Experiments on the role of water in petroleum formation. *Geochimica et Cosmochimica Acta* **61**, 3691-3723.
- Lin, L. H., Wang, P. L., Rumble, D., Lippmann-Pipke, J., Boice, E., Pratt, L. M., Lollar, B. S., Brodie, E. L., Hazen, T. C., Andersen, G. L., DeSantis, T. Z., Moser, D. P., Kershaw, D., and Onstott, T. C., (2006) Long-term sustainability of a high-energy, low-diversity crustal biome. *Science* **314**, 479-482.
- Lippmann, J., Stute, M., Torgersen, T., Moser, D. P., Hall, J. A., Lin, L., Borcsik, M., Bellamy, R. E. S., and Onstott, T. C., (2003) Dating ultra-deep mine waters with noble gases and ³⁶Cl, Witwatersrand Basin, South Africa. *Geochimica et Cosmochimica Acta* **67**, 4597-4619.
- Liu, Q. and Liu, S., (1999) Magnetic and mineralogical characteristics of reservoir rocks in the Yakela oil field, northern Tarim Basin and their implications for magnetic detection of oil and gas accumulations. *Chinese Science Bulletin* **44**, 174-177.
- Liu, Q. Y., Dai, J. X., Li, J., and Zhou, Q. H., (2008) Hydrogen isotope composition of natural gases from the Tarim Basin and its indication of depositional environments of the source rocks. *Sci. China Ser. D-Earth Sci.* **51**, 300-311.
- Martin, G., (1993) Pyrolysis of organosulfur compounds. In: *Supplement S: The chemistry of Sulphur-containing functional groups*, pp395-437. Patai, S. and Rappoport, Z. (Ed.). Wiley.
- McCollom, T. M. and Seewald, J. S., (2001) A reassessment of the potential for reduction of dissolved CO₂ to hydrocarbons during serpentinization of olivine. *Geochimica et Cosmochimica Acta* **65**, 3769-3778.
- McCollom, T. M. and Seewald, J. S., (2003a) Experimental constraints on the hydrothermal reactivity of organic acids and acid anions: I. Formic acid and formate. *Geochimica et Cosmochimica Acta* **67**, 3625-3644.

- McCollom, T. M. and Seewald, J. S., (2003b) Experimental study of the hydrothermal reactivity of organic acids and acid anions: II. Acetic acid, acetate, and valeric acid. *Geochimica et Cosmochimica Acta* **67**, 3645-3664.
- McCollom, T. M. and Seewald, J. S., (2007) Abiotic synthesis of organic compounds in deep-sea hydrothermal environments. *Chemical Reviews* **107**, 382-401.
- McCollom, T. M., Lollar, B. S., Lacrampe-Couloume, G., and Seewald, J. S., (2010) The influence of carbon source on abiotic organic synthesis and carbon isotope fractionation under hydrothermal conditions. *Geochimica et Cosmochimica Acta* **74**, 2717-2740.
- Ni, Y., Ma, Q., Ellis, G. S., Dai, J., Katz, B., Zhang, S., and Tang, Y., (2011) Fundamental studies on kinetic isotope effect (KIE) of hydrogen isotope fractionation in natural gas systems. *Geochimica et Cosmochimica Acta* **75**, 2696-2707.
- Nurmi, P. A., Kukkonen, I. T., and Lahermo, P. W., (1988) Geochemistry and origin of saline groundwaters in the Fennoscandian Shield. *Applied Geochemistry* **3**, 185-230.
- Onstott, T. C., Lin, L. H., Davidson, M., Mislowack, B., Borcsik, M., Hall, J., Slater, G., Ward, J., Lollar, B. S., Lippmann-Pipke, J., Boice, E., Pratt, L. M., Pfiffner, S., Moser, D., Gihring, T., Kieft, T. L., Phelps, T. J., Vanheerden, E., Litthaur, D., Deflaun, M., Rothmel, R., Wanger, G., and Southam, G., (2006) The origin and age of biogeochemical trends in deep fracture water of the Witwatersrand Basin, South Africa. *Geomicrobiology Journal* **23**, 369-414.
- Oremland, R. S., Miller, L. G., and Whiticar, M. J., (1987) Sources and flux of natural gases from Mono Lake, California. *Geochimica et Cosmochimica Acta* **51**, 2915-2929.
- Palmer, D. A. and Drummond, S. E., (1986) Thermal decarboxylation of acetate. Part I. The kinetics and mechanism of reaction in aqueous solution *Geochimica et Cosmochimica Acta* **50**, 813-823.

- Proskurowski, G., Lilley, M. D., Kelley, D. S., and Olson, E. J., (2006) Low temperature volatile production at the Lost City Hydrothermal Field, evidence from a hydrogen stable isotope geothermometer. *Chemical Geology* **229**, 331-343.
- Proskurowski, G., Lilley, M. D., Seewald, J. S., Fruh-Green, G. L., Olson, E. J., Lupton, J. E., Sylva, S. P., and Kelley, D. S., (2008) Abiogenic hydrocarbon production at Lost City hydrothermal field. *Science* **319**, 604-607.
- Reynolds, R. L., Fishman, N. S., Wanty, R. B., and Goldhaber, M. B., (1990) Iron sulfide minerals at Cement oil field, Oklahoma: Implications for magnetic detection of oil fields. *Geological Society of America Bulletin* **102**, 368-380.
- Sachse, D., Radke, J., and Gleixner, G., (2006) ~~D values of individual~~ plants along a climatic gradient - Implications for the sedimentary biomarker record. *Organic Geochemistry* **37**, 469-483.
- Sackett, W. M., (1978) Carbon and hydrogen isotope effects during thermo-catalytic production of hydrocarbons in laboratory simulation experiments. *Geochimica et Cosmochimica Acta* **42**, 571-580.
- Schefuss, E., Schouten, S., and Schneider, R. R., (2005) Climatic controls on central African hydrology during the past 20,000 years. *Nature* **437**, 1003-1006.
- Schimmelmann, A., Lewan, M. D., and Wintsch, R. P., (1999) D/H isotope ratios of kerogen, bitumen, oil, and water in hydrous pyrolysis of source rocks containing kerogen types I, II, IIS, and III. *Geochimica et Cosmochimica Acta* **63**, 3751-3766.
- Schimmelmann, A., Boudou, J. P., Lewan, M. D., and Wintsch, R. P., (2001) Experimental controls on D/H and $^{13}\text{C}/^{12}\text{C}$ ratios of kerogen, bitumen and oil during hydrous pyrolysis. *Organic Geochemistry* **32**, 1009-1018.
- Schimmelmann, A., Sessions, A. L., Boreham, C. J., Edwards, D. S., Logan, G. A., and Summons, R. E., (2004) D/H ratios in terrestrially sourced petroleum systems. *Organic Geochemistry* **35**, 1169-1195.

- Schimmelmann, A., Sessions, A. L., and Mastalerz, M., (2006) Hydrogen isotopic (D/H) composition of organic matter during diagenesis and thermal maturation. *Annu. Rev. Earth Planet. Sci.* **34**, 501-533.
- Schmidt, K., Koschinsky, A., Garbe-Schonberg, D., de Carvalho, L. M., and Seifert, R., (2007) Geochemistry of hydrothermal fluids from the ultramafic-hosted Logatchev hydrothermal field, 15°N on the Mid-Atlantic Ridge: Temporal and spatial investigation. *Chemical Geology* **242**, 1-21.
- Schoell, M., (1983) Genetic characterization of natural gases. *AAPG Bulletin* **67**, 546-546.
- Seewald, J. S., (1994) Evidence for metastable equilibrium between hydrocarbons under hydrothermal conditions. *Nature* **370**, 285-287.
- Seewald, J. S., (1997) Mineral redox buffers and the stability of organic compounds under hydrothermal conditions. *Mat. Res. Soc. Symp. Proc.* **412**, 317-331.
- Seewald, J. S., (2001a) Aqueous geochemistry of low molecular weight hydrocarbons at elevated temperatures and pressures: Constraints from mineral buffered laboratory experiments. *Geochimica et Cosmochimica Acta* **65**, 1641-1664.
- Seewald, J. S., (2001b) Model for the origin of carboxylic acids in basinal brines. *Geochimica et Cosmochimica Acta* **65**, 3779-3789.
- Seewald, J. S., (2003) Organic-inorganic interactions in petroleum-producing sedimentary basins. *Nature* **426**, 327-333.
- Seewald, J. S., Zolotov, M. Y., and McCollom, T., (2006) Experimental investigation of single carbon compounds under hydrothermal conditions. *Geochimica et Cosmochimica Acta* **70**, 446-460.
- Sessions, A. L., Sylva, S. P., Summons, R. E., and Hayes, J. M., (2004) Isotopic exchange of carbon-bound hydrogen over geologic timescales. *Geochimica et Cosmochimica Acta* **68**, 1545-1559.

- Sessions, A. L. and Hayes, J. M., (2005) Calculation of hydrogen isotopic fractionations in biogeochemical systems. *Geochimica Et Cosmochimica Acta* **69**, 593-597.
- Sessions, A. L., (2006) Isotope-ratio detection for gas chromatography. *J. Sep. Sci.* **29**, 1946-1961.
- Seyfried, W., Gordon, P. C., and Dickson, F. W., (1979) A new reaction cell for hydrothermal solution equipment. *American Mineralogist* **64**, 646-649.
- Seyfried, W., D.R. Janecky and M.E. Berndt, (1987) Rocking autoclaves for hydrothermal experiments II: The flexible reaction-cell system. In: *Hydrothermal Experimental Techniques*, pp216-239. Ulmer, G. C. and Barnes, H. L. (Ed.). Wiley, New York.
- Seyfried, W. and Ding, K., (1995) Phase equilibria in subseafloor hydrothermal systems: a review of the role of redox, temperature, pH and dissolved Cl on the chemistry of hot spring fluids at mid-ocean ridges. In: *Seafloor Hydrothermal Systems: Physical, Chemical, Biological, and Geological Interactions*, pp248-272. Humphris, S. E., Zierenberg, R. A., Mullineaux, L. S., and Thomson, R. E. (Ed.). American Geophysical Union.
- Seyfried, W., Foustoukos, D. I., and Allen, D. E., (2004) Ultramafic-hosted hydrothermal systems at Mid-Ocean Ridges: Chemical and physical constraints on pH, redox, and carbon reduction reactions. In: *Mid-Ocean Ridges: Hydrothermal Interactions between the Lithosphere and Oceans*, pp267-285. German, C., Lin, J., and Parson, L. (Ed.). American Geophysical Union.
- Seyfried, W., Pester, N. J., Ding, K., and Rough, M., (2011) Vent fluid chemistry of the Rainbow hydrothermal system (36°N, MAR): Phase equilibria and in situ pH controls on subseafloor alteration processes. *Geochimica et Cosmochimica Acta* **75**, 1574-1593.
- Sherwood, B., Fritz, P., Frappe, S. K., Macko, S. A., Weise, S. M., and Welhan, J. A., (1988) Methane occurrences in the Canadian Shield. *Chemical Geology* **71**, 223-236.
- Sherwood Lollar, B., Frappe, S. K., Fritz, P., Macko, S. A., Welhan, J. A., Blomqvist, R., and Lahermo, P. W., (1993a) Evidence for bacterially generated hydrocarbon gas in Canadian

- Shield and Fennoscandian Shield rocks. *Geochimica et Cosmochimica Acta* **57**, 5073-5085.
- Sherwood Lollar, B., Frapce, S. K., Weise, S. M., Fritz, P., Macko, S. A., and Welhan, J. A., (1993b) Abiogenic methanogenesis in crystalline rocks. *Geochimica et Cosmochimica Acta* **57**, 5087-5097.
- Sherwood Lollar, B., Weise, S. M., Frapce, S. K., and Barker, J. F., (1994) Isotopic constraints on the migration of hydrocarbon and helium gases of southwestern Ontario. *Bulletin of Canadian Petroleum Geology* **42**, 283-295.
- Sherwood Lollar, B., Westgate, T. D., Ward, J. A., Slater, G. F., and Lacrampe-Couloume, G., (2002) Abiogenic formation of alkanes in the Earth's crust as a minor source for global hydrocarbon reservoirs. *Nature* **416**, 522-524.
- Sherwood Lollar, B., Lacrampe-Couloume, G., Slater, G. F., Ward, J., Moser, D. P., Gihring, T. M., Lin, L. H., and Onstott, T. C., (2006) Unravelling abiogenic and biogenic sources of methane in the Earth's deep subsurface. *Chemical Geology* **226**, 328-339.
- Sherwood Lollar, B., Lacrampe-Couloume, G., Voglesonger, K., Onstott, T. C., Pratt, L. M., and Slater, G. F., (2008) Isotopic signatures of CH₄ and higher hydrocarbon gases from Precambrian Shield sites: A model for abiogenic polymerization of hydrocarbons. *Geochimica et Cosmochimica Acta* **72**, 4778-4795.
- Shock, E. L. and Helgeson, H. C., (1990) Calculation of the thermodynamic and transport properties of aqueous species at high pressures and temperatures: Standard partial molal properties of organic species. *Geochimica et Cosmochimica Acta* **54**, 915-945.
- Shock, E. L., (1992) Chemical environments of submarine hydrothermal systems. *Orig. Life Evol. Biosph.* **22**, 67-107.
- Siskin, M., Brons, G., Katritzky, A. R., and Balasubramanian, M., (1990) Aqueous Organic Chemistry .1. Aquathermolysis - Comparison with Thermolysis in the Reactivity of Aliphatic Compounds. *Energy & Fuels* **4**, 475-482.

- Surdam, R. C. and Crossey, L. J., (1985) Organic inorganic reactions during progressive burial: Key to porosity and permeability enhancement and preservation. *Philosophical Transactions of the Royal Society of London Series A-Mathematical Physical and Engineering Sciences* **315**, 135-156.
- Tang, Y. C., Huang, Y. S., Ellis, G. S., Wang, Y., Kralert, P. G., Gillaizeau, B., Ma, Q. S., and Hwang, R., (2005) A kinetic model for thermally induced hydrogen and carbon isotope fractionation of individual n-alkanes in crude oil. *Geochimica et Cosmochimica Acta* **69**, 4505-4520.
- Tang, Y. C., Ellis, G. S., and Ma, Q. S., (2007) Use of carbon and hydrogen stable isotopic composition to quantitatively assess natural gas generation. *Geochimica et Cosmochimica Acta* **71**, A1001 (abstr.). 17th Annual V. M. Goldschmidt Conference, Cologne, Germany, August 2007.
- Tissot, B. P. and Welte, D. H., (1984) *Petroleum Formation and Occurrence*. 2nd Ed. Springer-Verlag.
- Toulmin, P., III and Barton, P. B., Jr., (1964) A thermodynamic study of pyrite and pyrrhotite. *Geochimica et Cosmochimica Acta* **28**, 641-671.
- Wang, Y. and Sessions, A. L., (2008) Memory effects in compound-specific D/H analysis by gas chromatography/pyrolysis/isotope-ratio mass spectrometry. *Analytical Chemistry* **80**, 9162-9170.
- Wang, X. B., Guo, Z. Q., Tuo, J. C., Guo, H. Y., Li, Z. X., Zhuo, S. G., Jiang, H. L., Zeng, L. W., Zhang, M. J., Wang, L. S., Liu, C. X., Yan, H., Li, L. W., Zhou, X. F., Wang, Y. L., Yang, H., and Wang, G., (2009a) Abiogenic hydrocarbons in commercial gases from the Songliao Basin, China. *Sci. China Ser. D-Earth Sci.* **52**, 213-226.
- Wang, Y., Sessions, A., Nielsen, R. J., and Goddard, W. A., III, (2009b) Equilibrium $^2\text{H}/^1\text{H}$ fractionations in organic molecules: I. Experimental calibration of ab initio calculations. *Geochimica et Cosmochimica Acta* **73**, 7060-7075.

- Wang, Y., Sessions, A., Nielsen, R. J., and Goddard, W. A., III, (2009c) Equilibrium $^2\text{H}/^1\text{H}$ fractionations in organic molecules. II: Linear alkanes, alkenes, ketones, carboxylic acids, esters, alcohols and ethers *Geochimica et Cosmochimica Acta* **73**, 7076-7086.
- Ward, J. A., Slater, G. F., Moser, D. P., Lin, L. H., Lacrampe-Couloume, G., Bonin, A. S., Davidson, M., Hall, J. A., Mislouck, B., Bellamy, R. E. S., Onstott, T. C., and Lollar, B. S., (2004) Microbial hydrocarbon gases in the Witwatersrand Basin, South Africa: Implications for the deep biosphere. *Geochimica et Cosmochimica Acta* **68**, 3239-3250.
- Weres, O., Newton, A. S., and Tsao, L., (1988) Hydrous pyrolysis of alkanes, alkenes, alcohols and ethers. *Organic Geochemistry* **12**, 433-444.
- Whiticar, M. J., Faber, E., and Schoell, M., (1985) Hydrogen and carbon isotopes of C_1 to C_5 alkanes in natural gases. *AAPG Bulletin* **69**, 316 (abstr.).
- Whiticar, M. J., (1990) A geochemical perspective of natural gas and atmospheric methane. *Organic Geochemistry* **16**, 531-547.
- Zhang, T. W., Amrani, A., Ellis, G. S., Ma, Q. S., and Tang, Y. C., (2008) Experimental investigation on thermochemical sulfate reduction by H_2S initiation. *Geochimica et Cosmochimica Acta* **72**, 3518-3530.